PROTEINS: Structure, Function, and Genetics 18:161–173 (1994)

The Structure of *Trypanosoma cruzi* Trypanothione Reductase in the Oxidized and NADPH Reduced State

Christina B. Lantwin,[1] Ilme Schlichting,[1] Wolfgang Kabsch,[1] Emil F. Pai,[2] and R. Luise Krauth-Siegel[3]
[1]Abteilung Biophysik, Max-Planck-Institut für Medizinische Forschung, D-69120 Heidelberg, Germany;
[2]Departments of Biochemistry and Molecular and Medical Genetics, University of Toronto, Toronto, Ontario M5S 1A8, Canada; and [3]Institut für Biochemie II, Universität Heidelberg, D-69120 Heidelberg, Germany

ABSTRACT **The three-dimensional structure of trypanothione reductase (TR) (EC 1.6.4.8) from *Trypanosoma cruzi* has been solved at 0.33 nm resolution by molecular replacement using the structure of *C. fasciculata* TR as a starting model. Elucidation of the *T. cruzi* TR structure represents the first step in the rational design of a drug against Chagas' disease. The structure of *T. cruzi* TR is compared with those of *C. fasciculata* TR as well as human and *E. coli* glutathione reductase (GR). In the FAD-binding domain, TR has two insertions, each about 10 residues long, which do not occur in GR. The first one is a rigid loop stabilizing the position of helix 91–117 which is responsible for the wider active site of TR as compared to GR. The second insertion does not occur where it is predicted by sequence alignment; rather the residues extend three strands of the 4-stranded β-sheet by one or two residues each. This increases the number of hydrogen bonds within the sheet structure. The structure of the NADPH·TR complex has been solved at 0.33 nm resolution. The nicotinamide ring is sandwiched between the flavin ring and the side chain of Phe-198 which undergoes the same conformational change upon coenzyme binding as Tyr-197 in GR. In addition to Arg-222 and Arg-228, which are conserved in TR and GR, Tyr-221—the last residue of the second β-sheet strand of the βαβ dinucleotide binding fold—is in hydrogen bonding distance to the 2′ phosphate group of NADPH.**

Key words: X-ray crystallography, disulfide oxidoreductases, FAD, NADPH, drug target, Chagas' disease

INTRODUCTION

Trypanosomes and leishmanias are the causative agents of African sleeping sickness (*Trypanosoma brucei gambiense, T. b. rhodesiense*), Nagana cattle disease (*T. b. brucei, T. b. congolense*), Chagas' disease (American trypanosomiasis, *T. cruzi*), Kala-azar (human visceral leishmaniasis, *Leishmania donovani*), and oriental sore (human cutaneous leishmaniasis, *L. tropica*). Besides other metabolic peculiarities, these parasitic protozoa possess a unique thiol metabolism.[1] In contrast to nearly all other eucaryotes and procaryotes[2,3] they lack the enzyme glutathione reductase. Their main thiols are covalent conjugates of glutathione and spermidine, namely monoglutathionylspermidine and bis(glutathionyl)spermidine [trypanothione, $T(SH)_2$[4]]. These compounds are kept reduced by the enzyme trypanothione reductase (TR):

$$TS_2 + NADPH + H^+ \overset{TR}{\rightleftharpoons} T(SH)_2 + NADP^+ .$$

Trypanothione reductase has been purified from *Crithidia fasciculata*[5] and from *T. cruzi*.[6] The genes of *T. congolense* TR[7] and *T. cruzi* TR[8] have been cloned and expressed in *E. coli*. The enzyme is a representative of the FAD-cystine-oxidoreductases[9–11] as are glutathione reductase (GR), lipoamide dehydrogenase, and mercuric ion reductase.

T. cruzi TR shares many physical and chemical properties with GR, the closest related host enzyme. The most important difference between both enzymes is their exclusive specificity towards their disulfide substrate.[6] The known sensitivity of the parasite against oxidative stress[12] together with the finding that its defense mechanisms rely on the trypanothione system make *T. cruzi* TR a most attractive target for the development of a drug against Chagas' disease. Comparative kinetic studies with several inhibitors in solution indicate that a selective inhibition of TR should be possible.[13,14] The structural differences between *T. cruzi* TR and human GR could be exploited in the design of a specific

Abbreviations: GR, glutathione reductase (EC 1.6.4.2); GSSG, glutathione disulfide; Gsp_{ox}, monoglutathionylspermidine disulfide; TR, trypanothione reductase (EC 1.6.4.8); TS_2, trypanothione disulfide; $T(SH)_2$, reduced trypanothione [N^1,N^8-bis(glutathionyl)spermidine]; rms, root mean square; 1 Å = 0.1 nm; Tris, tris(hydroxymethyl)aminomethane; residues with primed numbers belong to the other subunit.

Received July 6, 1993; revision accepted September 21, 1993.
Address reprint requests to R. Luise Krauth-Siegel, Institut für Biochemie II, Im Neuenheimer Feld 328, D-69120 Heidelberg, Germany.

TABLE I. Statistics of Crystallographic Data*

		Resolution shells			
	Overall	∞–8.0	8.0–6.0	6.0–4.0	4.0–3.3
Native crystal					
No. of measured reflections	88764	10767	14704	35034	28259
No. of unique reflections	41811	3300	4503	17453	16525
No. of possible reflections	46716	3410	4518	18428	20360
R^*(%)	12.7	5.7	11.6	12.6	24.3
Completeness (%) of all the data	89.5	97.7	99.7	94.7	81.2
Data with $I/\sigma > 1$		95.1	92.7	81.3	57.5
Data with $I/\sigma > 3$		89.2	72.0	51.7	18.1
$R^\dagger$(%) using data with $I/\sigma > 1$	(20.6)	51.3	28.4	18.9	22.5
NADPH soaked crystal					
No. of measured reflections	63485	7656	10589	24686	20554
No. of unique reflections	39078	2768	4067	16158	16085
R^*(%)	15.7	7.6	16.4	16.5	27.7
Completeness (%) of all the data	83.7	81.2	90.0	87.7	79.0
Data with $I/\sigma > 1$		79.1	84.3	74.8	56.5
Data with $I/\sigma > 3$		72.9	63.3	46.5	17.1
$R^\dagger$(%) using data with $I/\sigma > 1$	(22.5)	45.6	29.3	20.3	25.1

*$R = \Sigma_h\Sigma_i|I_{hi} - I_h|/\Sigma_{hi}I_{hi}$ where h are unique reflection indices and I_{hi} are the intensities of symmetry equivalent reflections giving a mean value of I_h.

†$R = \Sigma|F_{obs} - F_{model}|/\Sigma F_{obs}$ where F_{obs} and F_{model} are observed and model structure factor amplitudes, respectively. No bulk solvent correction has been applied to the data. The overall R-factors given in parentheses include only data between 8 and 3.3 Å resolution.

inhibitor of the parasite enzyme. The structure of human glutathione reductase is known at 1.54 Å resolution.[15] So far the three-dimensional structures of two TRs from the insect parasite *C. fasciculata* have been solved.[16,17] The sequence identity between *C. fasciculata* and *T. cruzi* TR is 69%, indicating similar overall structures. Since even single amino acid substitutions can strongly influence the binding of a substrate or inhibitor, the structure of the authentic target molecule should offer the best guidance for the design of a specific inhibitor. Here we describe the three-dimensional structures of *T. cruzi* trypanothione reductase in its oxidized and 2-electron-reduced state. The binding of the dinucleotide substrate NADPH is shown. The structures are compared with those of *C. fasciculata* TR[16,17] and human GR.[15,18]

MATERIALS AND METHODS

Crystals and Data Collection

Purification and crystallization of *T. cruzi* TR were carried out as described.[19] The crystals were difficult to grow reproducibly and those obtained show relatively poor internal order. Structure determination is based on the monoclinic crystals (space-group $P2_1$, $a = 136.3$ Å, $b = 91.1$ Å, $c = 126.0$ Å, $\beta = 94.0°$) grown from 1.2 M sodium citrate, 20 mM Tris, 1 mM EDTA, pH 8.0 in the presence of 2% octanoyl-*N*-methylglucamide. The asymmetric unit contains two dimers of *T. cruzi* TR, each subunit comprising 492 amino acid residues and a tightly bound FAD molecule.

Reduced trypanothione reductase (EH_2·NADPH) crystals were obtained by soaking a crystal of the oxidized enzyme (0.25 × 0.3 × 1.2 mm^3) with 25 mM NADPH in 1.4 M sodium citrate, 20 mM Tris, 1 mM EDTA, pH 8.0 for 10 min at room temperature in the absence of octanoyl-*N*-methylglucamide. The presence of detergent is essential for crystal growth but not necessary for crystal storage or soaking. Reduction of the enzyme was followed visually by the color change from bright yellow to orange-red. The crystal was mounted in a capillary completely filled with the soaking solution to prevent reoxidation and was fixed by cotton fibers from pipe cleaners.

All X-ray diffraction data were recorded on an electronic area detector (Siemens/Nicolet/Madison WI) at 4°C. The crystal-to-detector distance was 13 cm. X-rays (CuK_α) were generated using a GX-18 rotating anode (Elliot/Enraf-Nonius, Delft) and focused by Franks double mirror optics. The anode was operated at 35 kV and 50 mA. Camera and detector were controlled by a simplified version of a program by Blum et al.[20] Data frames were processed by the program XDS.[21–23] A native and an NADPH-soaked data set, each from one crystal, were collected to an effective resolution of 3.3 Å. The detailed statistics of each data set are shown in Table I.

Structure Determination

The three-dimensional structure of trypanothione reductase from *T. cruzi* was determined by molecular replacement using the *C. fasciculata* TR coordinates[16] of the dimer as the starting model.

Orientation and position of the starting model

with respect to our monoclinic unit cell were obtained using the molecular replacement routines from the program package XPLOR.[24,25] The model was placed in a 100 Å × 100 Å × 100 Å cubic box and a Patterson map was calculated. This map was rotated to find the best agreements with the Patterson map obtained from the measured intensities. Four crystallographically independent peaks of the correlation function were found. They were between 2.6 and 2.9 standard deviations above the mean. The peaks A and B as well as A′ and B′ are each related by a rotation of 84° about the crystallographic 2-fold axis. The same rotation has been found also as the highest noncrystallographic peak (correlation factor 0.4) in the self-rotation map derived from the measured intensities of the native data set. Detailed analysis of the four peaks has revealed that the positions of the peaks A′ and B′ are consequences of the 2-fold rotation by which the two molecules in the dimeric search model are related. Hence, the monoclinic crystals contain two dimers corresponding to the peaks A and B in the asymmetric unit. The search model of the dimer was rotated by the Eulerian angles $\theta_1 = 347°$, $\theta_2 = 54°$, $\theta_3 = 89°$ into the orientation corresponding to peak A in the cross-rotation map. The position of the rotated dimer was found at 0.32a + 0.129c using the method of Fujinaga and Read,[26] as implemented in the XPLOR program package.

The component along the *b*-axis was set to zero since it is arbitrary in the monoclinic space group. The same procedure was repeated for the second dimer corresponding to peak B. After a rotation by the Eulerian angles $\theta_1 = 168°$, $\theta_2 = 30°$, $\theta_3 = 269°$ the second dimer was moved around while the first dimer was kept fixed. A unique peak of 11σ above the mean was found at 0.914*a* + 0.734*b* + 0.964*c*. The solution of the molecular replacement problem thus obtained was found acceptable as judged by visual inspection of the model using the interactive graphics program FRODO[27] adapted to an IRIS 4GT (Silicon Graphics Inc., Mountain View, CA) by C.M. Cambillau. The side chains of the model were corrected according to the amino acid sequence of *Trypanosoma cruzi* trypanothione reductase.[8]

The resulting *T. cruzi* TR model was refined using the program XPLOR,[24,25] thereby imposing strict noncrystallographic constraints between the four monomers in the asymmetric unit because of the limited number of available data (Table I) in the resolution range 10–3.3 Å. The crystallographic *R*-factor which measures the agreement between computed and observed structure factor amplitudes as defined in the footnote to Table I was reduced from an initial value of 47 to 34% by least-squares minimization. Further progress was obtained by a number of rounds of molecular dynamics refinement using the standard protocol for heating, fast cooling, and minimization.[28] After each round phase information from the refined model was combined with the observed structure factor amplitudes in a way similar to the method of Read[29] which reduces model bias in the new electron density map. The fit between the refined atomic model and the new density map was inspected and improved manually using the program FRODO.[27] A final crystallographic *R*-factor of 20.6% was obtained after a number of rounds of refinement and rebuilding. Individual isotropic temperature factors were determined as the final step of the refinement. Variations of temperature factors of covalently bonded atoms were restrained to 1.5 and 2.0 Å^2 for main chain and side chain atoms, respectively. Additional target restraints of 2.0 Å^2 (main chain) and 2.5 Å^2 (side chain) were imposed on the temperature factors of atoms related by bond angles. In the refined structure the variations of the temperature factors of bonded atoms are found to exceed their target values by a factor of 1.13; for atoms related by bond angles the variations are larger by a factor of 1.29. The mean value of all temperature factors is 17.1 Å^2. The root-mean-square (rms) deviations of the bond lengths and bond angles from ideality[30] are 0.01 Å and 1.3°, respectively. Most of the main chain dihedral angles are within the allowed regions of the Ramachandran plot (Fig. 1). All others correspond to residues in loop regions. The estimated error of atomic positions as derived from a Luzzati plot is 0.35 Å.[31]

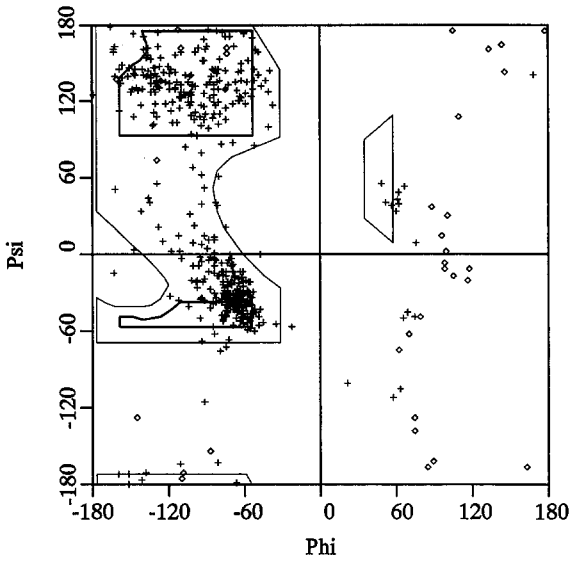

Fig. 1. Ramachandran plot of main chain torsion angles φ and ψ. ◇ and + represent glycines and all other residues, respectively.

The structure of the complex between *T. cruzi* TR and NADPH was determined by the difference Fourier technique since the unit cell constants were identical with the native ones. Readily interpretable

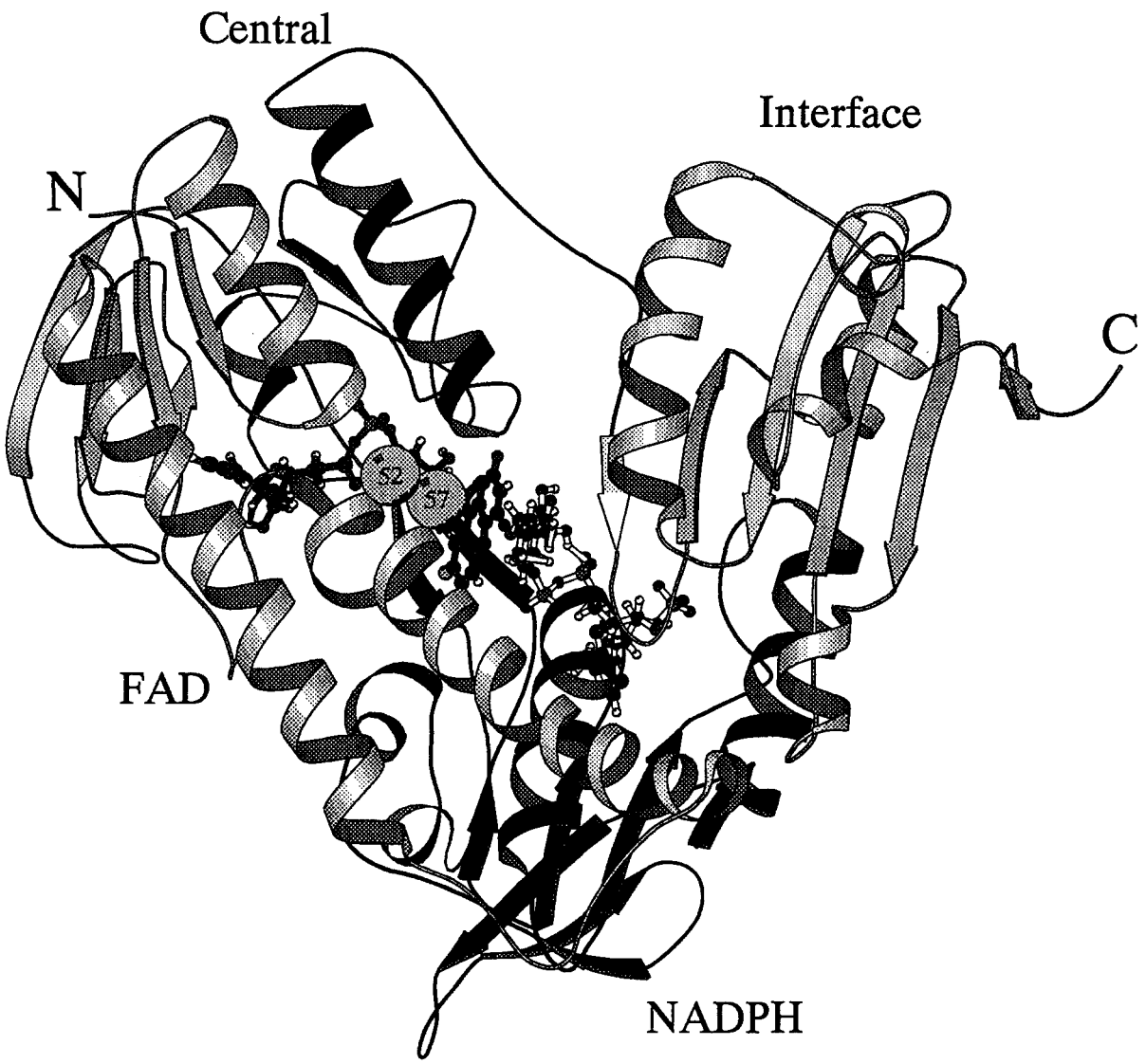

Fig. 2. Ribbon diagram[32] of one subunit of the homodimeric trypanothione reductase. Arrows depict β-strands; α-helices are shown as spirals. The FAD domain and the interface domain are shaded light, whereas the NADPH domain and the central domain are shaded darker. The spheres represent the sulfur atoms of Cys-52 and Cys-57, the active site thiols. The cofactors FAD and NADPH are shown as ball-and-stick models with dark and light shading, respectively.

electron density was found at the expected binding site of NADPH supporting the correctness of the structure. In each subunit of the dimer an atomic model of NADPH was fitted to the electron density. This structure was refined as described above for the native structure. The final crystallographic R-factor for the 29,088 unique reflections for $F > \sigma$ between 8.0 and 3.3 Å was 22.5%. Again good model geometry was observed, with (rms) bond length and dihedral angle deviations of 0.009 Å and 1.3°, respectively.

RESULTS AND DISCUSSION

The three-dimensional structure of trypanothione reductase from *T. cruzi* has been solved by molecular replacement using the structure of *C. fasciculata* TR[16] as a model.

Both subunits of the homodimeric flavoprotein can be subdivided into four domains: the FAD domain (residues 1–160), the NADPH domain (residues 161–290), the central domain (residues 291–360), and the interface domain (residues 361–492) (Fig. 2). The dimeric flavoenzyme has two identical active sites, each being formed by residues of both subunits. The structure of *T. cruzi* TR closely resembles that of *C. fasciculata* TR and also that of human GR. 69% of all amino acid residues in *T. cruzi* TR are identical with those in the *C. fasciculata* enzyme[8,33] (Table II). The even higher sequence identity of 79% between the enzymes from *T. cruzi*[8] and *T. congo-*

TABLE II. Sequence Identities and rms Deviations of *T. cruzi* TR, *C. fasciculata* TR, and Human GR*

	T. cruzi TR	*C. fasciculata* TR	Human GR
T. cruzi TR	—	0.7 Å (479)	1.7 Å (444)
C. fasciculata TR	69%	—	1.6 Å (446)
Human GR	32%	34%	—

*The values in parentheses are the number of equivalent residues.

lense[34] mirrors the closer phylogenetic relationship within the mammalian parasites in comparison to the insect parasite. The sequence identities between human GR[35] and TR from *T. cruzi*[8] and *C. fasciculata*[33] give no indication for a coevolution of host and parasite enzyme.

The structure of *T. cruzi* TR will be compared with the *C. fasciculata* TR structure of Kuriyan et al.[16]—which differs by only 2 amino acid substitutions from the second *C. fasciculata* TR structure[17]—and with the structure of human GR.[15] The two *cis*-peptide bonds observed in GR[15] are conserved in TR. They occur between Pro-369 and Pro-370, and between His-460 and Pro-461, respectively. In addition there is a *cis*-peptide unique to TRs between Pro-42 and Pro-43 in a loop which is missing in GR.

FAD Binding Domain

The 160 N-terminal residues form the FAD binding domain. It contributes the redox active couple Cys-52–Cys-57 to the catalytic site.

A striking difference between the structure of TR and GR is the more open active site of TR. This widening is due to rotations of the first and third helix (residues 13–27 and 91–117) of the FAD domain. Within the TRs the structural orientation of both helices and the sequence of the first one are highly conserved. At the C-terminal ends of the helices, Lys-28 and Glu-118 are conserved in all TRs but not in GR. In *T. cruzi* TR the distance between NZ of Lys-28 and OE2 of Glu-118 is 3.0 Å. This interaction may contribute to the relative orientation of the two helices. In the third α-helix (91–117) several amino acid residues are different in TR from *T. cruzi*[8] and *C. fasciculata*.[33] All of these residues are directed into a solvent channel. Residues pointing into the disulfide substrate binding cavity (Ile-106, Ser-109, Tyr-110, Met-113) are conserved.

The most obvious structural differences between TR and GR are two insertions, both about 10 residues in length, within the FAD domain of TR. Their structures but not their sequences (Tables III and IV, Fig. 3) are highly conserved. The first insertion consisting of predominantly hydrophobic residues (residues 39–47 in *T. cruzi* TR, between position 53 and 54 of human GR) occurs just in front of the active site sequence which is conserved in all FAD-cystine-oxidoreductases.[9] It forms a rigid loop structure due to the cis-peptide bond between Pro-42 and Pro-43 and internal hydrogen bonds between the main chain atoms of residues 41 and 45 (Fig. 4). The structure of the loop as well as its accessibility to solvent are amazingly similar in *T. cruzi* and *C. fasciculata* TR although only 5 out of 9 residues are identical (Table III). In *T. cruzi* TR the polar Ser-46 is poorly accessible to solvent. Instead, its hydroxyl-group is within hydrogen bonding distance to the ribose oxygens of FAD. Comparing the residues which surround the loop with the corresponding residues in GR reveals that only Gln-37 (His-52 in GR) and Tyr-183 (Gln-182 in GR) are exchanged. Both amino acids which are conserved within the TRs form hydrogen bonds with several main chain atoms of the loop. In addition, His-40 of the loop is in hydrogen bond distance to Asp-100 and Asn-107. As these residues are part of the third α-helix (91–117) this interaction could contribute to orient the helix away from the active site.

TABLE III. Solvent Accessibilities of the First Long Insertion of Trypanothione Reductases*

T. cruzi TR

	Residue number								
	39	40	41	42	43	44	45	46	47
Sequence	Val	His	Gly	Pro	Pro	Phe	Phe	Ser	Ala
Accessibility (Å^2)	63	29	4	87	84	71	21	14	0
Secondary structure	S	S	B	T	T	T	B	—	—

C. fasciculata TR

	Residue number								
	38	39	40	41	42	43	44	45	46
Sequence	His	His	Gly	Pro	Pro	His	Tyr	Ala	Ala
Accessibility (Å^2)	91	28	1	74	93	68	35	9	0
Secondary structure	S	S	B	T	T	T	B	—	—

*The accessibilities and the secondary structural assignments were determined using the program DSSP.[37] B, bridge; S, bend; T, turn.

According to sequence alignment[33] the second major insertion in TR (residues 131–140) (Table IV) occurs between residues 133 and 134 of GR. It is therefore expected to be located in the first bend between two antiparallel β-strands (Fig. 3). Contrary to this expectation only the first two residues (Ser-131 and Lys-132) of the insertion are found there whereas the next 7 residues (Asn-133 to Glu-139) are incorporated in the second β-strand. The last inserted residue (Ser-140) is found in the β-bend between the second and third β-strand. The residues expected from sequence alignment to be in the sec-

TABLE IV. Structural Alignment of the Second Long Insertion in *T. cruzi* TR and *C. fasciculata* TR With Human GR*

	T. cruzi TR									
	Residue number									
	131	132	133	134	135	136	137	138	139	140
Sequence	Ser	Lys	Asn	Val	Val	Asn	Val	Arg	Glu	Ser
Secondary structure	S	S	S	E	E	E	E	E	S	S
	C. fasciculata TR									
	Residue number									
	130	131	132	133	134	135	136	137	138	139
Sequence	Asp	Asn	His	Thr	Val	Leu	Val	Arg	Glu	Ser
Secondary structure	E	T	T	E	E	E	E	E	S	S
	Human GR									
	Residue number									
	138	139	140	141	142	143				
Sequence	Pro	Thr	Ile	Glu	Val	Ser				
Secondary structure	—	E	E	E	E	T				

*Secondary structure was assigned using the program DSSP.[37] The structural alignment of this section does not coincide with the best sequence alignment which inserts the additional residues between residue 133 and 134 of human GR.[33] For further details see Figure 3 and the text. E, extended; S, bend; T, turn.

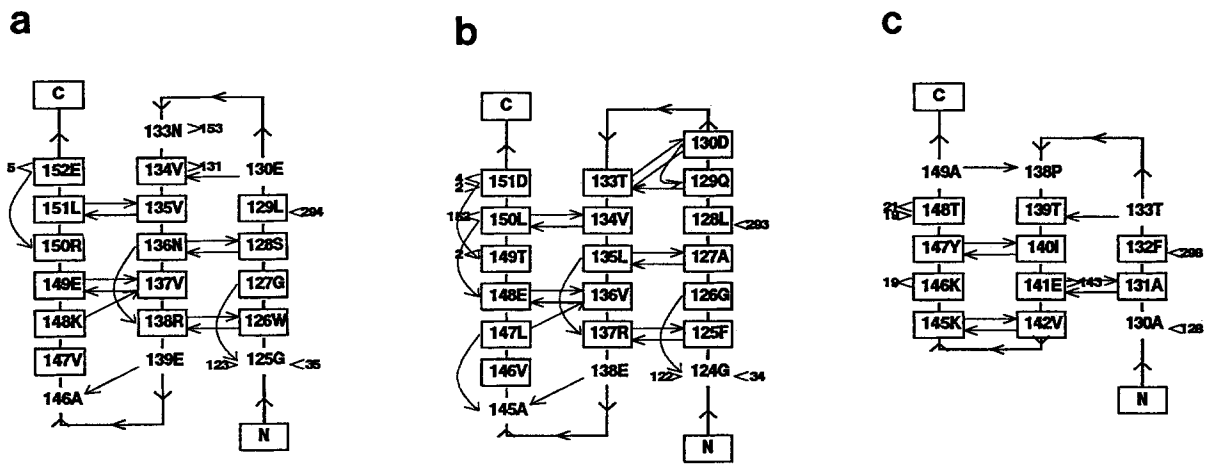

Fig. 3. Hydrogen bonding diagram[36,37] of three strands of the 4-stranded β-sheet in the FAD domain of (**a**) *T. cruzi* TR, (**b**) *C. fasciculata* TR, and (**c**) human GR. The insertion residues (131–140 in *T. cruzi* TR, see Table IV) contribute to the extension of the sheet structure with significantly more hydrogen bond pairings in TR (a and b) than in GR (c). The best sequence alignment would have placed the additional residues between residues 133 and 134 of human GR (for details see text).

ond β-strand are shifted into the next turn where they form the second additional loop not present in the GR structure. Comparing the hydrogen bonding diagrams between TR and GR shows that the β-sheet is conserved, but that the individual strands are longer by one or two residues which results in additional hydrogen bonds in the TR structures (Fig. 3a–c). In conclusion, the second stretch of additional residues in TR significantly extends the β-pleated sheet in the FAD domain and is therefore expected to play a major role for structural stability.

FAD binds to TR in the same extended conformation as to human GR.[15] Nearly all amino acid residues interacting with the prosthetic group are conserved between TR and GR (Table V). In contrast to NADPH where the adenine ring does not make any direct contact with the protein, N1 of the adenine ring of FAD is fixed by a backbone nitrogen as in GR.[15] Hydrogen bonds between the adenine ring and the protein may be important for the discrimination against flavinmononucleotide.

O2′ and O3′ of the ribose are in hydrogen bond distance to the side chain carboxylate of Asp-35 at the C-terminal end of the second strand of the

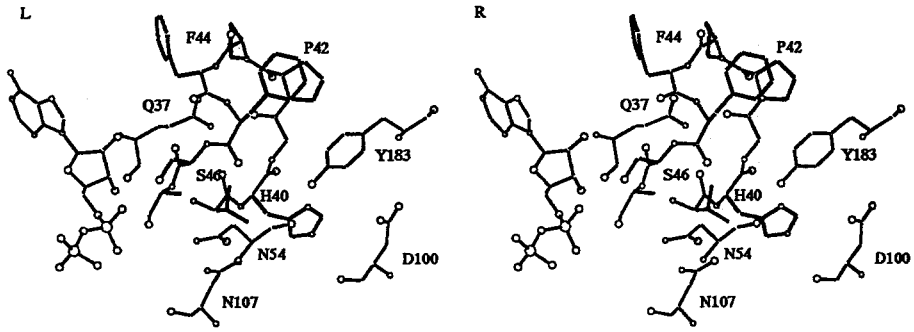

Fig. 4. Structure of the insertion (residues 39–47) in *T. cruzi* TR together with surrounding residues, and the adenine ribose pyrophosphate moiety of FAD. The backbone structure of the loop is almost identical with that in *C. fasciculata* TR[16] although only 5 out of 9 residues are identical (Table III). It is very rigid due to internal hydrogen bonds and to the *cis*-peptide bond between Pro-42 and Pro-43. The interactions of the conserved His-40 with Asp-100 and Asn-107 probably stabilize the position of the helix 91–117.

β-sheet in the FAD binding Rossmann fold. An acidic residue at this position is conserved in nearly all adenyl ribose-binding proteins.[38,39] In *T. cruzi* TR O2′ and O3′ are also in hydrogen bond distance to Ser-46, which is part of the first long insertion (Fig. 4).

The pyrophosphate moiety of the cofactor is bound at the loop between the first strand of the β-sheet and the following α-helix (residues 13–27) of the Rossmann fold. The negative charges of the pyrophosphate are partially compensated by the dipole moment of the helix.[40] OF1 forms the typical hydrogen bond with the nitrogen of Gly-15, which is the second peptide unit of the dinucleotide binding helix. OF2 forms a hydrogen bond with the main chain nitrogen of Asp-326 again analogous to human GR (Table V). All protein residues surrounding the ribityl chain, a characteristic part of flavin nucleotides, are conserved among the known TR and GR sequences.

The xylene moiety of the flavin ring does not make any direct contact with the protein. The 7α-methyl group points into a hydrophobic pocket formed by Phe-182, Phe-203, and Ile-199. The nearest neighbor to the 8α-methyl group is the side chain of Arg-287. The catalytically active pteridine moiety is tightly bound by hydrogen bonds between N3 and the carbonyl oxygen of His-460′, and between O2α and the nitrogen of Thr-334, the first residue of the α-helix (334–348) in the central domain. The dipole moment of the helix[40] is assumed to stabilize the negative charge at O2α which might develop during catalysis.[41] The hydrogen bond between O4α of the isoalloxazine and the side chain of Lys-60 is also conserved in GR (Table V).

Disulfide Substrate Binding Site

The active site is formed by residues of the FAD, NADPH, and central domain of one monomer and the interface domain of the other monomer. The binding sites for the disulfides TS_2 or Gsp_{ox} and for NADPH are spacially separated by the isoalloxazine ring of FAD (Fig. 5). This geometry is characteristic for all FAD-cystine-oxidoreductases.[9–11]

The assumed trypanothione binding site resembles that for GSSG in GR with the redox-active Cys-52–Cys-57 couple and the isoalloxazine ring at its center. In the outer region this site is much wider in TR than in GR due to a different orientation of the helices 13–27 and 91–117 in the FAD domain. Since binding of trypanothione to TR crystals has not yet been successful the probable binding mode of TS_2 has been deduced[16,17] from the known binding of GSSG to human GR.[42,43] Only 5 out of 19 residues in GR surrounding the bound GSSG[42] are not identical or homologous in TR (Table VI). Together with Asn-22 which replaces Arg-38, in total three arginine residues in human GR are exchanged by neutral or acidic residues in TR. These alterations take into account the different charges of the disulfide substrates, −2 in GSSG compared to +1 and +4 in TS_2 and Gsp_{ox}, respectively. Site-directed mutageneses with the aim to exchange the substrate specificities of TR and GR[44–46] revealed the residues corresponding to Glu-18 and Trp-21 in TR to be crucial for substrate specificity. According to these experiments it seems easier to adapt a GR to reduce TS_2 than a TR to reduce GSSG. This finding is supported by the fact that *E. coli* GR reduces GSSG as well as TS_2.[45] The lower substrate specificity of the bacterial enzyme may be correlated to a main chain deviation observed between *E. coli* and human GR[47] which coincides with the start of the first insertion in TR (Table III, Fig. 4). Since in the GR·GSSG complex the substrate forms 10 direct but also 14 solvent-mediated polar interactions with the protein,[43] the more open active site of TR probably prevents tight binding of the smaller GSSG molecule.

Residues which are conserved in all TRs as well as *E. coli* GR but not in human GR may also play a role in the binding of TS_2 without discriminating against GSSG. As a point in case, the polar side

TABLE V. Residues Within 3.5 Å Distance to the Prosthetic Group FAD in *T. cruzi* TR*

FAD atom	*T. cruzi* TR Atom	(residue)	Distance(Å)	Human GR[15] Atom	(residue)†	Distance(Å)
Adenine ring						
N1	N	(Gly-127)	2.9	N	(Ala-130)	2.9
Ribose						
O2′	NH2	(Arg-290)	3.4		(Asn-294)	
O2′	OG	(Ser-46)	3.4		‡	
O2′	OD2	(Asp-35)	3.4	OE2	(Glu-50)	2.65
O3′	OG	(Ser-46)	2.6		‡	
O3′	OD1	(Asp-35)	2.8	OE1	(Glu-50)	2.69
O3′	OD2	(Asp-35)	3.2		(Glu-50)	
O4′	OD1	(Asp-35)	3.4		(Glu-50)	
Pyrophosphate group						
OA1	OG1	(Thr-51)	2.8	OG1	(Thr-57)	2.85
OA2	N	(Ser-14)	3.2		(Ser-30)	
OA2	N	(Thr-51)	3.1	N	(Thr-57)	3.16
OA2	O4′	(flavin)	3.2	O4′	(flavin)	2.96
O5′	OD2	(Asp-326)	3.2		(Asp-331)	
OF2	N	(Asp-326)	3.1	N	(Asp-331)	2.97
OF1	N	(Ser-14)	3.3		(Ser-30)	
OF1	N	(Gly-15)	2.9	N	(Gly-31)	2.74
Ribityl chain						
O3′	OD1	(Asp-326)	3.1		(Asp-331)	
O3′	OD2	(Asp-326)	3.0	OD2	(Asp-331)	2.76
O3′	N	(Leu-333)	3.5			
Flavin ring						
N1	SG	(Cys-57)	3.5		(Cys-63)	
O2α	N	(Thr-334)	3.1	N	(Thr-339)	3.10
N3	O	(His-460′)	3.2	O	(His-467′)	2.74
N3	SG	(Cys-57)	3.3		(Cys-63)	
O4α	NZ	(Lys-60)	2.7	NZ	(Lys-66)	2.78
N5	NZ	(Lys-60)	3.2	NZ	(Lys-66)	3.01
$8\alpha CH_3$	NH2	(Arg-287)	3.5	NE	(Arg-291)	

*The distances were taken from the structural model at 3.3 Å resolution. The distances in GR are derived from the structure at 1.54 Å resolution.[15]

†When distances have not been reported only the corresponding amino acid residue is given.

‡There is no corresponding residue due to the 9 amino acid residues long insertion in TR between residue 53 and 54 of GR.

chain of Ser-109 preceding the highly conserved Tyr-110 (Table VI) is directed into the active site cleft and is a candidate for substrate interaction. Trp-21 and Met-113, also close to the tyrosine-110 ring, have been discussed to form a hydrophobic patch which repels the Gly I carboxylate of GSSG.[17] Since in *E. coli* GR the corresponding residues are Asn-21 and Val-102[48] it is unlikely that Met-113 plays a role in the discrimination against GSSG. In addition, it should be emphasized that Ser-109, Tyr-110, and Met-113 in TR are far more distant from the active site disulfide than the corresponding residues in human GR because they are constituents of the differently oriented α-helix. Upon binding of the larger glutathionylspermidines they may interact with the spermidine(s). In conclusion, predicting the precise binding mode of trypanothione disulfide to TR is not possible solely on the GSSG-GR structure because the majority of polar interactions between GSSG and GR is solvent mediated[43] and because the binding of glutathionyl conjugates can be influenced strongly by the nonglutathione moiety.[49] In addition, Arg-347, which interacts with one of the glutamyl moieties of GSSG, is replaced by Ala-342 in TR. This exchange may be necessary for sterical compensation due to the substitution of Ala-34 by Glu-18 in TR. Recently the structure of the complex between *C. fasciculata* TR and Gsp_{ox} has been solved.[50] As expected, one spermidine interacts with Glu-18, Trp-21, and Met-113. The second glutathionylspermidine moiety which is not as tightly bound to the protein is in close contact to the C_α-atom of Gly-112. In *T. cruzi* and *T. congolense* TR this position is occupied by an acidic residue which may have an influence on the binding of the disulfide substrates. Work is in progress to solve the structure of the TS_2·*T. cruzi* TR complex.

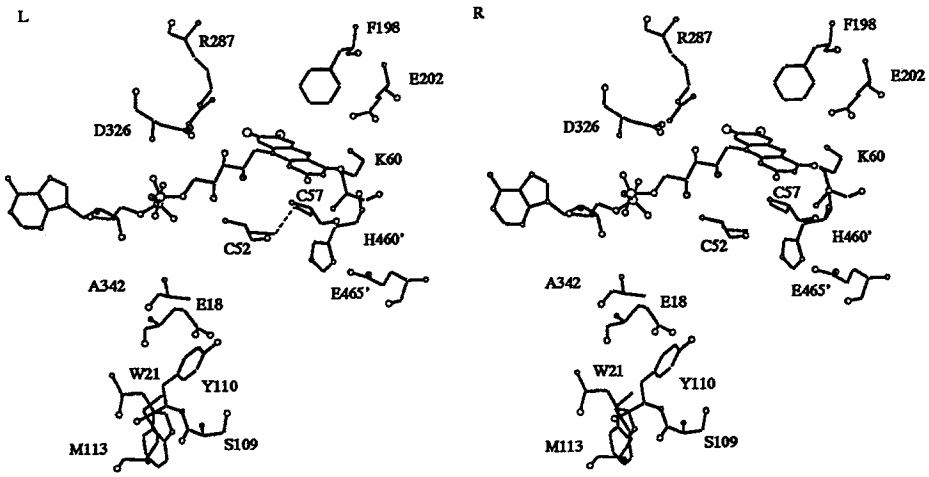

Fig. 5. Active site of *T. cruzi* TR. The isoalloxazine ring of FAD forms the center of the active site. ––– represents the active site disulfide bridge. His-460′ and Glu-465′ are residues of the other subunit. In the oxidized enzyme species the side chain of Phe-198 points nearly perpendicular onto the flavin ring.

TABLE VI. Residues around the GSSG Binding Site of Human GR Which Are *Not* Conserved in TR

T. cruzi TR*[8]	*E. coli* GR[46]	Human GR[42,43]	Interacting part of GSSG in human GR
Glu-18	Ala-18	Ala-34	Gly I
Trp-21	Asn-21	Arg-37	Gly I
Ser-109	Ser-98†	Ile-113	Gly II
Met-113	Val-102†	Asn-117	Gly II
Ala-342	Arg-319	Arg-347	Glu I

*All residues are identical in *T. congolense* and *C. fasciculata* TR.
†Since *E. coli* GR in contrast to human GR also reduces trypanothione disulfide the residues may be involved in the binding of this conjugate without influencing the binding of GSSG.

Structure With Bound NADPH

TR has a specific requirement for NADPH as reducing cofactor, the activity with NADH is only 3% of that with NADPH.[6] Binding of NADPH to TR crystals was achieved by soaking with 25 mM NADPH. Despite the high NADPH concentration no secondary binding site was observed.

The structure of the TR·NADPH complex will be compared with that of the GR·NADPH complex[51,52] since the binding mode of NADPH to *C. fasciculata* TR is not known. NADPH is bound to the protein in an extended conformation, the adenine and nicotinamide rings exhibiting anti conformation as in human GR[52] (Fig. 6). Most of its contacts are with residues of the NADPH domain (residues 161–290). The nicotinamide ring which is roughly coplanar to the flavin ring also interacts with residues of the FAD domain, and the central and the interface domain.

The adenine moiety of NADPH does not make any direct hydrogen bond to the protein. The nearest contact is to the main chain oxygen of Ile-285, 3.4 Å away from N7. Specific interactions are not necessary because there is no need to discriminate against other bases. The remaining part of the molecule has many contacts with the protein whereby most of the residues lining the NADPH binding pocket of TR are identical with those in GR (Table VII).

A characteristic part of the NADPH molecule is the 2′ phosphate group. Its oxygen atoms are fixed by the guanidinium groups of Arg-222 and Arg-228 (Fig. 7a). In the oxidized enzyme the side chain of Arg-222 has no clear electron density but binding of NADPH leads to its fixation as indicated by a sharp drop of the temperature factors of the guanidinium group atoms. The third residue within hydrogen bonding distance to the 2′ phosphate is Tyr-221 which is the last residue of the second strand of the βαβ fold. This residue plays a major role in the discrimination between NADH and NADPH binding.[35,39] In nearly all NAD-dependent enzymes the position is occupied by an acidic residue whereas human and *E. coli* GR possess a branched chain amino acid. Since Tyr-221 is conserved in the known TR sequences the binding mode observed in *T. cruzi* TR is a new variation of the theme.

In human GR the environment around the 2′ phosphate group is similar to that in TR since the Arg residues are conserved. In addition, His-219 occupies a similar position as Tyr-221 in TR (Fig. 7b). It should be emphasized that this structural coincidence is not accommodated by equivalent residues: Tyr-221 in TR precedes the first conserved Arg whereas His-219 in GR is C-terminal to this Arg residue.

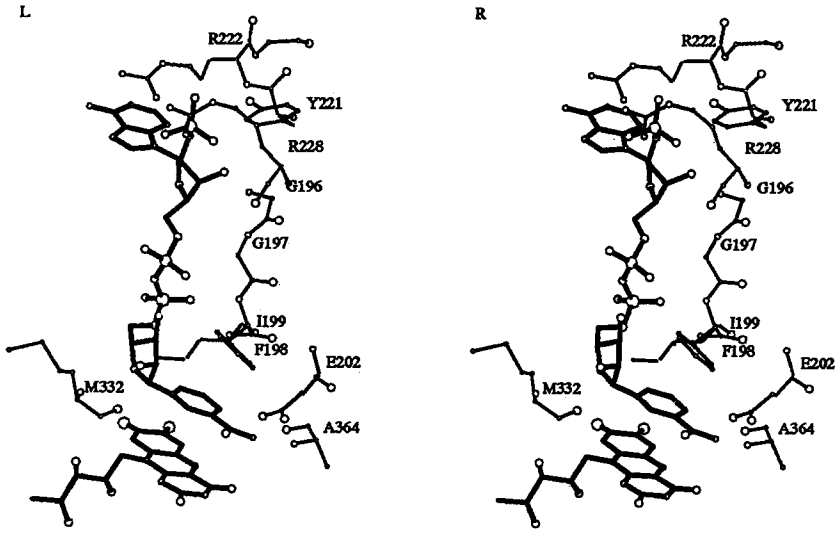

Fig. 6. Binding of NADPH to *T. cruzi* trypanothione reductase. The bound coenzyme is shown together with the residues within 3.5 Å of the NADPH molecule. In the structure of the reduced enzyme the aromatic ring systems of the flavin, the nicotinamide and Phe-198 form a coplanar array as in human GR.

TABLE VII. Residues Within 3.5 Å Distance to NADPH in the *T. cruzi* NADPH-TR Structure*

	T. cruzi TR			Human GR[40,49†]		
Atom of NADPH	Atom	(residue)	Distance (Å)	Atom	(residue)	Distance (Å)
Adenine ribose						
2′ phosphate O1	OH	(Tyr-221)	3.1		(Ile-217)	
2′ phosphate O1	NH2	(Arg-222)	2.6	NH1	(Arg-218)	3.0
2′ phosphate O2	NH2	(Arg-228)	2.9		(Arg-224)	
2′ phosphate O2	OH	(Tyr-221)	2.2		(Ile-217)	
2′ phosphate O3	NH2	(Arg-222)	3.1		(Arg-218)	
2′ phosphate O3	NH2	(Arg-228)	2.7	NE	(Arg-224)	2.8
O3′	N	(Gly-196)	3.2		(Ala-195)	
Pyrophosphate group						
A-phosphate O1	N	(Phe-198)	3.5	N	(Tyr-197)	3.5
N-phosphate O2	N	(Phe-198)	2.9		(Tyr-197)	
N-phosphate O2	N	(Ile-199)	2.9	N	(Ile-198)	3.0
Nicotinamide ribose						
O2′	O	(Met-332)	2.6	O	(Leu-337)	2.6
Nicotinamide						
O7	O	(Ala-364)	3.4	O	(Val-370)	
N7	OE2	(Glu-202)	3.0	OE1	(Glu-201)	2.6
N7	O	(Ala-364)	2.8	O	(Val-370)	2.9
N7	O4α	(flavin)	3.1			
C4	OE1	(Glu-202)	3.5		(Glu-201)	
C4	N5	(flavin)	3.4			

*The distances are taken from the structural model at 3.3 Å resolution. The distances in NADPH-GR are derived from the structure at 2.0 Å resolution.[43]

†When distances have not been reported only the corresponding residue is given.

As expected for the binding of dinucleotides[39,40] the pyrophosphate bridge of NADPH is fixed to the loop between the first β-sheet strand and the following α-helix (residues 198–210) of the Rossmann fold. The negative charges are partly compensated by the dipole moment of the helix.[40,53] No side chain atoms are involved in the binding of the pyrophosphate. The closest contacts are to backbone atoms of Phe-198, Ile-199, and Gly-286 (Table VII). The hydrogen bond to the amide of the third residue of the pyro-

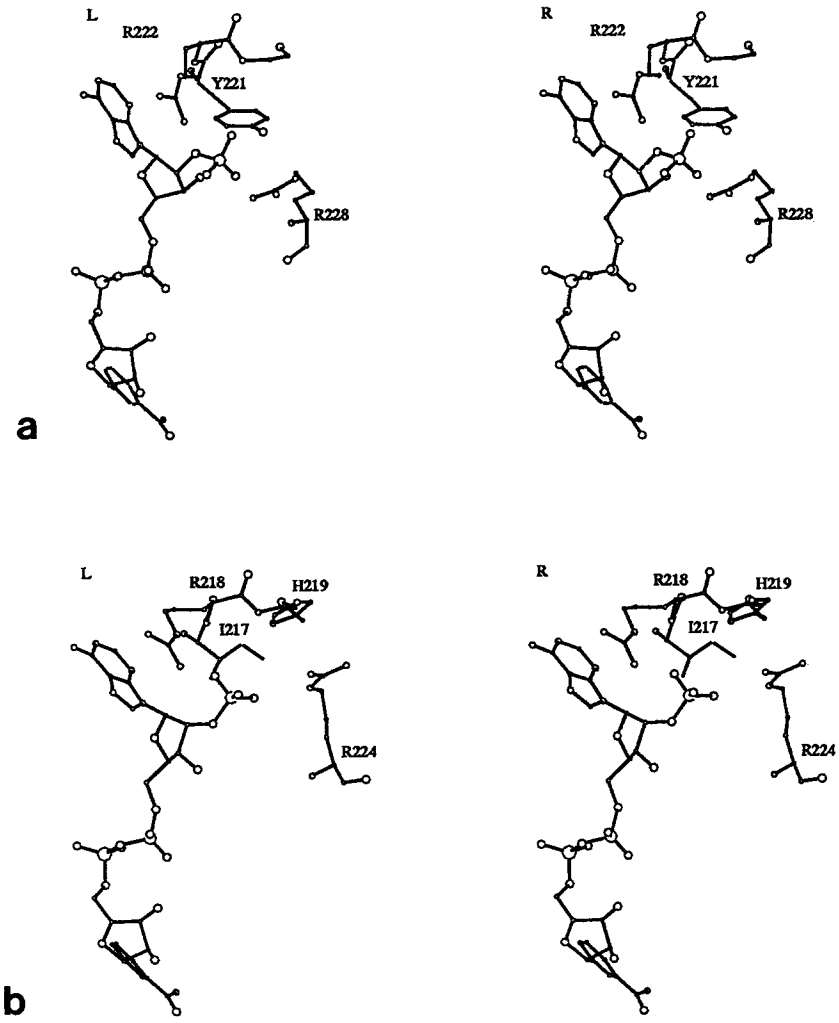

Fig. 7. Binding of the 2′ phosphate group of NADPH to (**a**) *T. cruzi* TR and (**b**) human GR. In both enzymes two arginine residues bind to the 2′ phosphate. The third residue interacting with the phosphate is Tyr-221 in TR and His-219 in GR, respectively. Note that these residues do not occupy equivalent sequence positions. Tyr-221 is the last residue of the second sheet strand of the βαβ fold which plays a crucial role in the discrimination between NADH or NADPH binding.[39] His-219 in GR is the residue C-terminal to the first conserved arginine and is part of the turn.

phosphate-binding α-helix (Ile-199) is a common feature of the nucleotide binding fold.[40]

The distance between the coplanar nicotinamide and flavin rings is about 3.5 Å. The amide group of NADPH has the closest contacts with the protein (Fig. 6; Table VII). It is within hydrogen bonding distance to Glu-202 which together with Lys-60 forms the highly conserved active site salt bridge. Reduction of *T. cruzi* TR by NADPH causes some structural changes of the active site. The most striking difference is the movement of Phe-198. In the oxidized enzyme the aromatic ring points nearly perpendicularly onto the flavin ring (Fig. 5) as it is the case for the corresponding Tyr residues in GR[51,52] and lipoamide dehydrogenase.[54] Binding of NADPH causes the side chain to assume a new position almost parallel to the nicotinamide and flavin rings (Fig. 6). In the human GR structure the corresponding Tyr-197 makes a similar movement whereby in this case the hydroxyl-group of the tyrosine in its new position forms a strong H-bond with Thr-369.[43] Since *T. cruzi* and *T. congolense* TR possess a phenylalanine instead of the tyrosine residue this hydrogen bond cannot be important for NADPH binding.

The conformation of the FAD molecule is almost identical in the oxidized and reduced structures, except for small changes within the ribityl chain. These alterations seem to be due to the reduction of the disulfide bond between Cys-52 and Cys-57 as not only the side chains but also the main chain atoms of the cysteine residues move upon reduction. In the reduced enzyme the distance between the sulfur atoms of Cys-52 and Cys-57 is 3.5 Å. The thiolate of Cys-57, 3.5 Å apart from N5, undergoes the charge transfer interaction with the flavin and is within

hydrogen bonding distance to the side chain of Thr-334. As outlined for NADPH·GR this orientation makes an interaction with His-460′, the active site base, less favorable.[9,43] This interpretation is supported by the finding that the histidine—which protonates the first liberated thiol group of the product—is slightly closer to Cys-52 than to Cys-57.

CONCLUSIONS

Elucidation of the three-dimensional structure of trypanothione reductase from *T. cruzi* represents the basis for the design of a more specific drug against Chagas' disease. Comparing this structure with those of *C. fasciculata* Tr and human GR elucidated the role that the two long insertions in TR might play in the protein structure. Sequence and structure alignments with *C. fasciculata* TR as well as human and *E. coli* GR revealed residues conserved in the TRs and *E. coli* GR but substituted in human GR, which might be crucial for substrate specificity. Since *E. coli* GR is not as specific as human GR but also reduces TS_2,[45] its structure might be expected to be intermediate between the structures of TRs and human GR. The TR·NADPH structure presented here is the first TR structure for which coenzyme binding has been shown. Disulfide substrate and inhibitor binding studies with this crystal form are in progress.

ACKNOWLEDGMENTS

We are extremely grateful to Dr. John Kuriyan, who provided us with the coordinates of *C. fasciculata* trypanothione reductase. We thank Dr. Christopher Walsh and Dr. Francis Sullivan for providing the *T. cruzi* TR clone, Dr. Georg Schulz for the coordinates of NADPH and glutathione complexed to glutathione reductase, and Dr. Heiner Schirmer for his continuous interest and support. Christian Sticherling and Ingrid Jöst are gratefully acknowledged for the crystallization of *T. cruzi* TR, Klaus Scheffzek for help with data collection of the NADPH soaked crystals, and Helga Alt for typing the manuscript. This work was supported by the Deutsche Forschungsgemeinschaft (DFG Kr 1242/1-1). Coordinates have been submitted to the Brookhaven protein data bank.

REFERENCES

1. Fairlamb, A.H. Novel biochemical pathways in parasitic protozoa. Parasitology 99:S93–112, 1989.
2. Meister, A. A brief history of glutathione and a survey of its metabolism and functions. In: "Glutathione, Chemical, Biochemical, and Medical Aspects, Part A." Dolphin, D., Poulson, R., Avramovic, O. (eds.). New York: Wiley, 1989: 1–48.
3. Schirmer, R.H., Krauth-Siegel, R.L., Schulz, G.E. Glutathione reductase. In: "Glutathione, Chemical, Biochemical and Medical Aspects, Part A." Dolphin, D., Poulson, R., Avramovic, O. (eds.). New York: John Wiley, & Sons, 1989:553–596.
4. Fairlamb, A.H., Blackburn, P., Ulrich, P., Chait, B.T., Cerami, A. Trypanothione: A novel bis(glutathionyl)spermidine cofactor for glutathione reductase in trypanosomatids. Science 227:1485–1487, 1985.
5. Shames, S.L., Fairlamb, A.H., Cerami, A., Walsh, C.T. Purification and characterization of trypanothione reductase from *Crithidia fasciculata,* a newly discovered member of the family of disulfide-containing flavoprotein reductases. Biochemistry 25:3519–3526, 1986.
6. Krauth-Siegel, R.L., Enders, B., Henderson, G.B., Fairlamb, A.H., Schirmer, R.H. Trypanothione reductase from *Trypanosoma cruzi.* Purification and characterization of the crystalline enzyme. Eur. J. Biochem. 164:123–128, 1987.
7. Sullivan, F.X., Shames, S.L., Walsh, C.T. Expression of *Trypanosoma congolense* trypanothione reductase in *Escherichia coli:* Overproduction, purification, and characterization. Biochemistry 28:4986–4992, 1989.
8. Sullivan, F.X., Walsh, C.T. Cloning, sequencing, overproduction and purification of trypanothione reductase from *Trypanosoma cruzi.* Mol. Biochem. Parasitol. 44:145–147, 1991.
9. Williams, C.H., Jr. Lipoamide dehydrogenase, glutathione reductase, thioredoxin reductase, and mercuric ion reductase—a family of flavoenzyme transhydrogenases. In: "Chemistry and Biochemistry of Flavoenzymes," Vol. III. Müller, F. (ed.). Boca Raton, FL: CRC Press, 1992:121–211.
10. Petsko, G.A. Enzyme evolution, Déjà vu all over again. Nature (London) 352:104–105, 1991.
11. Pai, E.F. Variations on a theme: the family of FAD-dependent NAD(P)H-(disulphide)-oxidoreductases. Current Opinion in Structural Biology 1:796–803, 1991.
12. Boveris, A., Sies, H., Martino, E.E., Docampo, R., Turrens, J.F., Stoppani, A.O.M. Deficient metabolic utilization of hydrogen peroxide in *Trypanosoma cruzi.* Biochem. J. 188: 643–648, 1980.
13. Krauth-Siegel, R.L., Lohrer, H., Bücheler, U.S., Schirmer, R.H. The antioxidant enzymes glutathione reductase and trypanothione reductase as drug targets. In: "Biochemical Protozoology." Coombs, G., North, M. (eds.). London: Taylor & Francis, 1991:493–505.
14. Jockers-Scherübl, M.C., Schirmer, R.H., Krauth-Siegel, R.L. Trypanothione reductase from *Trypanosoma cruzi.* Catalytic properties of the enzyme and inhibition studies with trypanocidal compounds. Eur. J. Biochem. 180:267–272, 1989.
15. Karplus, P.A., Schulz, G.E. Refined structure of glutathione reductase at 1.54 Å resolution. J. Mol. Biol. 195: 701–729, 1987.
16. Kuriyan, J., Kong, X.P., Krishna, T.S.R., Sweet R.M., Murgolo, N.J., Field, H., Cerami, A., Henderson, G.B. X-Ray structure of trypanothione reductase from *Crithidia fasciculata* at 2.4 Å resolution. Proc. Natl. Acad. Sci. U.S.A. 88:8764–8768, 1991.
17. Hunter, W.N., Bailey, S., Habash, J., Harrop, S.J., Helliwell, J.R., Aboagye-Kwarteng, T., Smith, K., Fairlamb, A.H. Active site of trypanothione reductase. A target for rational drug design. J. Mol. Biol. 227:322–333, 1992.
18. Schulz, G.E., Schirmer, R.H., Sachsenheimer, W., Pai, E.F. The structure of the flavoenzyme glutathione reductase. Nature (London) 273:120–124, 1978.
19. Krauth-Siegel, R.L., Sticherling, C., Jöst, I., Walsh, C.T., Pai, E.F., Kabsch, W., Lantwin, C.B. Crystallization and preliminary crystallographic analysis of trypanothione reductase from *Trypanosoma cruzi,* the causative agent of Chagas' disease. FEBS Lett. 317:105–108, 1993.
20. Blum, M., Metcalf, P., Wiley, D.C. A system for collection and on-line integration of X-ray diffraction data from a multiwire area detector. J. Appl. Crystallogr. 20:235–247, 1987.
21. Kabsch, W. Automatic indexing of rotation diffraction patterns. J. Appl. Crystallogr. 21:67–71, 1988.
22. Kabsch, W. Evaluation of single-crystal X-ray diffraction data from a position-sensitive detector. J. Appl. Crystallogr. 21:916–924, 1988.
23. Kabsch, W. Processing of rotation diffraction data from crystals of initially unknown symmetry and cell constants. J. Appl. Crystallogr., in press.
24. Brünger, A.T. Extension of molecular replacement: A new search strategy based on Patterson correlation refinement. Acta Crystallogr. A46:46–57, 1990.

25. Brünger, A.T. Solution of a Fab(26-10)/Digoxin complex by generalized molecular replacement. Acta Crystallogr. A47:195–204, 1991.
26. Fujinaga, M., Read, R.J. Experiences with a new translation-function program. J. Appl. Crystallogr. 20:517–521, 1987.
27. Jones, T.A. A graphics model building and refinement system for macromolecules. J. Appl. Crystallogr. 11:268–272, 1978.
28. Brünger, A.T., Kuriyan, J., Karplus, M. Crystallographic R-factor refinement by molecular dynamics. Science 235: 458–460, 1987.
29. Read, R.J. Improved Fourier coefficients for maps using phases from partial structures with errors. Acta Crystallogr. A42:140–149, 1986.
30. Engh, R.A., Huber, R. Accurate bond and angle parameters for X-ray protein structure refinement. Acta Crystallogr. A47:392–400, 1991.
31. Luzzati, V. Traitement statistique des erreurs dans la determination des structures cristallines. Acta Crystallogr. 5:802–810, 1952.
32. Kraulis, P.J. Molscript: a program to produce both detailed and schematic plots of protein structures. J. Appl. Crystallogr. 24:946–950, 1991.
33. Field, H., Cerami, A., Henderson, G.B. Cloning, sequencing and demonstration of polymorphism in trypanothione reductase from *Crithidia fasciculata*. Mol. Biochem. Parasitol. 50:47–56, 1992.
34. Shames, S.L., Kimmel, B.E., Peoples, O.P., Agabian, N., Walsh, C.T. Trypanothione reductase of *Trypanosoma congolense:* Gene isolation, primary sequence determination, and comparison to glutathione reductase. Biochemistry 27: 5014–5019, 1988.
35. Krauth-Siegel, R.L., Blatterspiel, R., Saleh, M., Schiltz, E., Schirmer, R.H., Untucht-Grau, R. Glutathione reductase from human erythrocytes. The sequences of the NADPH domain and of the interface domain. Eur. J. Biochem. 121: 259–267, 1982.
36. Hutchinson, E.G., Thornton, J.M. HERA-A program to draw schematic diagrams of protein secondary structures. Proteins 8:203–212, 1990.
37. Kabsch, W., Sander, C. Dictionary of protein secondary structure: Pattern recognition of hydrogen-bonded and geometrical features. Biopolymers 22:2577–2637, 1983.
38. Rossmann, M.G., Moras, D., Olsen, K.W. Chemical and biological evolution of a nucleotide-binding protein. Nature (London) 250:194–199, 1974.
39. Baker, P.J., Britton, K.L., Rice, D.W., Rob, A., Stillman, T.J. Structural consequences of sequence patterns in the fingerprint region of the nucleotide binding fold. Implications for nucleotide specificity. J. Mol. Biol. 228:662–671, 1992.
40. Wierenga, R.K., De Maeyer, M.C.H., Hol, W.G.J. Interaction of pyrophosphate moieties with α-helixes in dinucleotide binding proteins. Biochemistry 24:1346–1357, 1985.
41. Krauth-Siegel, R.L., Schirmer, R.H., Ghisla, S. FAD analogues as prosthetic groups of human glutathione reductase. Properties of the modified enzyme species and comparison with the active site structure. Eur. J. Biochem. 148:335–344, 1985.
42. Karplus, P.A., Pai, E.F., Schulz, G.E. A crystallographic study of the glutathione binding site of glutathione reductase at 0.3 nm resolution. Eur. J. Biochem. 178:693–703, 1989.
43. Karplus, P.A., Schulz, G.E. Substrate binding and catalysis by glutathione reductase as derived from refined enzyme: substrate crystal structures at 2 Å resolution. J. Mol. Biol. 210:163–180, 1989.
44. Bradley, M., Bücheler, U.S., Walsh, C.T. Redox enzyme engineering: Conversion of human glutathione reductase into a trypanothione reductase. Biochemistry 30:6124–6127, 1991.
45. Henderson, G.B., Murgolo, N.J., Kuriyan, J., Osapay, K., Kominos, D., Berry, A., Scrutton, N.S., Hinchliffe, N.W., Perham, R.N., Cerami, A. Engineering the substrate specificity of glutathione reductase toward that of trypanothione reduction. Proc. Natl. Acad. Sci. U.S.A. 88:8769–8773, 1991.
46. Sullivan, F.X., Sobolov, S.B., Bradley, M., Walsh, C.T. Mutational analysis of parasite trypanothione reductase: acquisition of glutathione reductase activity in a triple mutant. Biochemistry 19:2761–2767, 1991.
47. Ermler, U., Schulz, G.E. The three-dimensional structure of glutathione reductase from *Escherichia coli* at 3.0 Å resolution. Proteins 9:174–179, 1991.
48. Greer, S., Perham, R.N. Glutathione reductase from *Escherichia coli:* Cloning and sequence analysis of the gene and relationship to other flavoprotein disulfide oxidoreductases. Biochemistry 25:2736–2742, 1986.
49. Bilzer, M., Krauth-Siegel, R.L., Schirmer, R.H., Ackerboom, T.P., Sies, H., Schulz, G.E. Interaction of a glutathione S-conjugate with glutathione reductase. Kinetic and X-ray crystallographic studies. Eur. J. Biochem. 138: 373–378, 1984.
50. Bailey, S., Smith, K., Fairlamb, A.H., Hunter, W.N. Substrate interactions between trypanothione reductase and N^1-glutathionylspermidine disulphide at 2.8 nm resolution. Eur. J. Biochem. 213:67–75, 1993.
51. Pai, E.F., Schulz, G.E. The catalytic mechanism of glutathione reductase as derived from X-ray diffraction analyses of reaction intermediates. J. Biol. Chem. 258:1752–1757, 1983.
52. Pai, E.F., Karplus, P.A., Schulz, G.E. Crystallographic analysis of the binding of NADPH, NADPH fragments, and NADPH analogues to glutathione reductase. Biochemistry 27:4465–4474, 1988.
53. Krauth-Siegel, R.L., Jacoby, E., Lantwin, C.B. The 3-dimensional structure of trypanothione reductase from *Trypanosoma cruzi* as a basis for drug design against Chagas' disease. In: "Flavins and Flavoproteins." Yagi, K. (ed.). Berlin: Walter de Gruyter, 1993:258–268.
54. Mattevi, A., Obmolova, G., Sokatch, J.R., Betzel, C., Hol, W.G.J. The refined crystal structure of *Pseudomonas putida* lipoamide dehydrogenase complexes with NAD^+ at 2.45 Å resolution. Proteins 13:336–351, 1992.